Isotopic composition of atmospheric nitrate in a tropical marine boundary layer

Joel Savarino[a,1], Samuel Morin[b], Joseph Erbland[a], Francis Grannec[a], Matthew D. Patey[c], William Vicars[a], Becky Alexander[d], and Eric P. Achterberg[c]

[a]Centre National de la Recherche Scientifique/Université Joseph Fourier Grenoble, Laboratoire de Glaciologie et Géophysique de l'Environnement, 38402 St. Martin d'Hères, France; [b]Météo-France/Centre National de la Recherche Scientifique, Centre National de Recherches Météorologiques-Groupe d'études de l'Atmosphère Météorologique, Centre d'Étude de la Neige, 38400 St. Martin d'Hères, France; [c]School of Ocean and Earth Science, National Oceanography Centre Southampton, University of Southampton, Southampton SO14 3ZH, United Kingdom; and [d]Department of Atmospheric Sciences, University of Washington, Seattle, WA 98195-1640

Long-term observations of the reactive chemical composition of the tropical marine boundary layer (MBL) are rare, despite its crucial role for the chemical stability of the atmosphere. Recent observations of reactive bromine species in the tropical MBL showed unexpectedly high levels that could potentially have an impact on the ozone budget. Uncertainties in the ozone budget are amplified by our poor understanding of the fate of NO_x (= NO + NO_2), particularly the importance of nighttime chemical NO_x sinks. Here, we present year-round observations of the multiisotopic composition of atmospheric nitrate in the tropical MBL at the Cape Verde Atmospheric Observatory. We show that the observed oxygen isotope ratios of nitrate are compatible with nitrate formation chemistry, which includes the $BrNO_3$ sink at a level of ca. 20 $\pm$ 10% of nitrate formation pathways. The results also suggest that the N_2O_5 pathway is a negligible NO_x sink in this environment. Observations further indicate a possible link between the NO_2/NO_x ratio and the nitrogen isotopic content of nitrate in this low NO_x environment, possibly reflecting the seasonal change in the photochemical equilibrium among NO_x species. This study demonstrates the relevance of using the stable isotopes of oxygen and nitrogen of atmospheric nitrate in association with concentration measurements to identify and constrain chemical processes occurring in the MBL.

monitoring | oxidation | tropic | bromine chemistry | aerosols

The tropical marine lower troposphere is one of the most photochemically active compartments of the global atmosphere. The year-round high solar radiation, temperature, and humidity render this region the second largest contributor to methane removal via the OH sink (1). A large proportion of tropospheric ozone loss also occurs in the tropical marine boundary layer (MBL), where the concentrations of precursors, such as NO_x (= NO + NO_2) and volatile organic carbons (VOCs) (2), are generally too low to keep the ozone production rate above its destruction rate. The destruction of ozone is further highlighted by the recently discovered role of halogen chemistry at low latitudes (3), which is known to destroy ozone catalytically (4). The subtle oxidation chemistry coupling NO_x, halogens, and VOCs with ozone production and destruction in the MBL is still not fully understood, as demonstrated by the historically overlooked bromine chemistry (3) or the role of heterogeneous N_2O_5 hydrolysis as a NO_x sink (5, 6).

Being the end product of the NO_x/O_3/VOC interaction, atmospheric nitrate is particularly well suited to probe such chemistry, especially through its stable isotope composition (7). Indeed, isotopic measurements have proven to be instrumental in identifying and quantifying sources, processes affecting the formation of atmospheric nitrate [particulate NO_3^- plus gas-phase nitric acid (HNO_3); hereafter defined as NO_3^-], and the role of its precursors (i.e., the complex chemical interactions between NO_x, halogens, and ozone) (8–10). Combining the analysis of the two stable oxygen isotope ratios ($^{17}O/^{16}O$ and $^{18}O/^{16}O$ expressed as $\delta^{17}O$ and $\delta^{18}O$, respectively) with the stable nitrogen isotope ratio ($^{15}N/^{14}N$ expressed as $\delta^{15}N$) in a single sample is a powerful tool that can

offer unique insights into atmospheric chemistry (11–14). The isotopic oxygen ratios of atmospheric NO_3^- are usually interpreted in the context of ^{17}O-excess ($\Delta^{17}O$), which is a more robust indicator of oxidation pathways forming NO_3^- than only δ values (15). $\Delta^{17}O(NO_3^-)$ serves as an integrator of the oxidation pathways (7) involving the main atmospheric oxidants (NO_3, OH, HO_2, and O_3; Fig. S1 and SI Text) and could provide both qualitative and quantitative constraints on the chemical reaction mechanisms leading to NO_3^- production (12, 13, 16–18). Nonzero values of $\Delta^{17}O(NO_3^-)$ stem directly from ozone, which possesses a characteristic ^{17}O-excess that is transferred during chemical reactions, whereas other oxidants involved in nitrate production possess $\Delta^{17}O$ values not significantly different from zero (15). The use of oxygen isotopes in nitrate is thus an emerging new tool that can be used to probe the oxidation capacity of the atmosphere, complementing the concentration measurements.

The interpretation of $\delta^{15}N(NO_3^-)$ is less well established. Variations in $\delta^{15}N(NO_3^-)$ can be interpreted, according to Freyer et al. (19), as resulting from changes in the source strength of reactive nitrogen (e.g., ref. 20) or as the result of isotope fractionation induced by transport, kinetic, or equilibrium atmospheric effects (21), with interpretation depending on regional atmospheric contexts.

To date, nitrate isotopes have been successfully used to assess atmospheric chemical processes in polar and midlatitude regions (10), but subtropical and tropical regions have not yet been studied extensively despite their strong oxidative conditions. Observational data would be useful for atmospheric chemistry modeling because these isotopic tracers provide constraints for chemical and physical models and constitute new markers for poorly constrained parameterizations (18). Furthermore, there is currently a lack of long-term observations of the oxidation capacity of the tropical MBL in NO_x-poor environments (22).

To address these gaps, we present a full seasonal cycle of nitrate isotope variations during the period July 2007 to July 2008 at the Cape Verde Atmospheric Observatory (CVAO; 16° 85′ N and 24° 87′ W, 50 m from the coastline and 10 m above sea level), situated in a region that is characteristic of the tropical oceanic boundary layer. The CVAO was established as an atmospheric observatory in 2006. Intensive and long-term studies conducted at the CVAO have already been reported (e.g., 23), and this well-characterized site allows for a thorough evaluation of the isotopic composition of nitrate in terms of the chemical state and physical state of the tropical MBL. This study combines seasonal variations of $\Delta^{17}O$ and $\delta^{15}N$ in the tropical MBL.

Results

Fig. 1 shows a seasonal time series of the atmospheric concentrations of NO_3^- and its $\Delta^{17}O$ and $\delta^{15}N$ values as recorded between July 2007 and July 2008. Data are also presented for aerosol samples collected in the vicinity of Cape Verde during various south–north Atlantic transects onboard the R/V *Polarstern*.

Nitrate concentration did not exhibit any apparent seasonal cycle during the study period. Concentrations were stable, averaging 21.4 ± 10.9 nmol·m^{-3}, consistent with the predominance of northeasterly trade winds at the CVAO, which supply a mixture of background marine air and polluted continental outflow (23). In contrast, $\Delta^{17}O$ and $\delta^{15}N$ displayed marked seasonal cycles that were somewhat out of phase. Maximum $\Delta^{17}O$ values occurred in winter ($\simeq30‰$), and minimum values occurred in summer ($\simeq26‰$). The $\delta^{15}N$ trend showed maximum values in spring ($-2.9‰$) and minimum values in fall ($-8.8‰$). For all variables, there is a very good agreement between the fixed (CVAO) and shipboard (i.e., R/V *Polarstern*) sample data. No correlations were found between atmospheric NO_3^- concentrations and isotope ratios.

Table 1 compares the CVAO observations with those from other northern hemisphere locations. From the pole to the tropics, the seasonality of $\Delta^{17}O$ shows a similar trend, with maximum values in winter and minimum values in summer. The amplitude is notably reduced in the tropics ($4‰$ compared with $>8‰$), principally due to relatively higher summer values. The $\Delta^{17}O$ values observed for the CVAO are the highest summer values ever reported for NO_3^- (up to $26‰$ on average) (Table 1). For $\delta^{15}N$, there is no common trend in terms of phase or maximum/minimum values compared with other studies (19, 24–26), preventing any general hemispheric

scale interpretations. We observed no common trend between $\delta^{15}N$ and NO_x concentrations. Also, no correlation was found between $\Delta^{17}O$ and $\delta^{15}N$, dismissing a common process for these two isotope markers, in contrast to observations made in the Arctic (26). Therefore, $\delta^{15}N$ was apparently not controlled by the termination reactions leading to the production of nitrate from NO_2. The only relationship that was noticeable between $\delta^{15}N$ and its precursor molecules was a positive correlation with the NO_2/NO_x ratio (Fig. 1C), in contrast to the negative trend observed for polluted air masses with high NO_x concentrations (19). A possible explanation would be a kinetic isotope effect between NO and NO_2, but in the absence of a better constrained system, $\delta^{15}N$ will not be further discussed because its interpretation will be too speculative.

As shown in Fig. 1 predicted nitrate aerosol concentrations and their corresponding $\Delta^{17}O$ values were calculated using a steady-state atmospheric chemistry box model [steady-state model (SSM), gray line] constrained by local measurements of NO, NO_2, O_3, $J(O^1D)$, and aerosol surface area (Table S1) and a 3D chemical transport model (CTM) GEOS-Chem (18) (gray dashed line). The SSM and CTM both predicted nearly identical nitrate aerosol concentrations but underestimated the observations by a factor of 2 (≈10 nmol·m^{-3} predicted and ≈20 nmol·m^{-3} observed). For $\Delta^{17}O$, a better agreement with observations was obtained with the SSM compared with the CTM, particularly for the summer values. The CTM was unable to reproduce the high summer $\Delta^{17}O$ values. Fig. 2 (see also Table S2) shows the different chemistries used by the different models, with DMS (CH_3SCH_3) being the main atmospheric sink of NO_3 (detailed information on the models and data reductions can be found in *Materials and Methods* and *SI Text*).
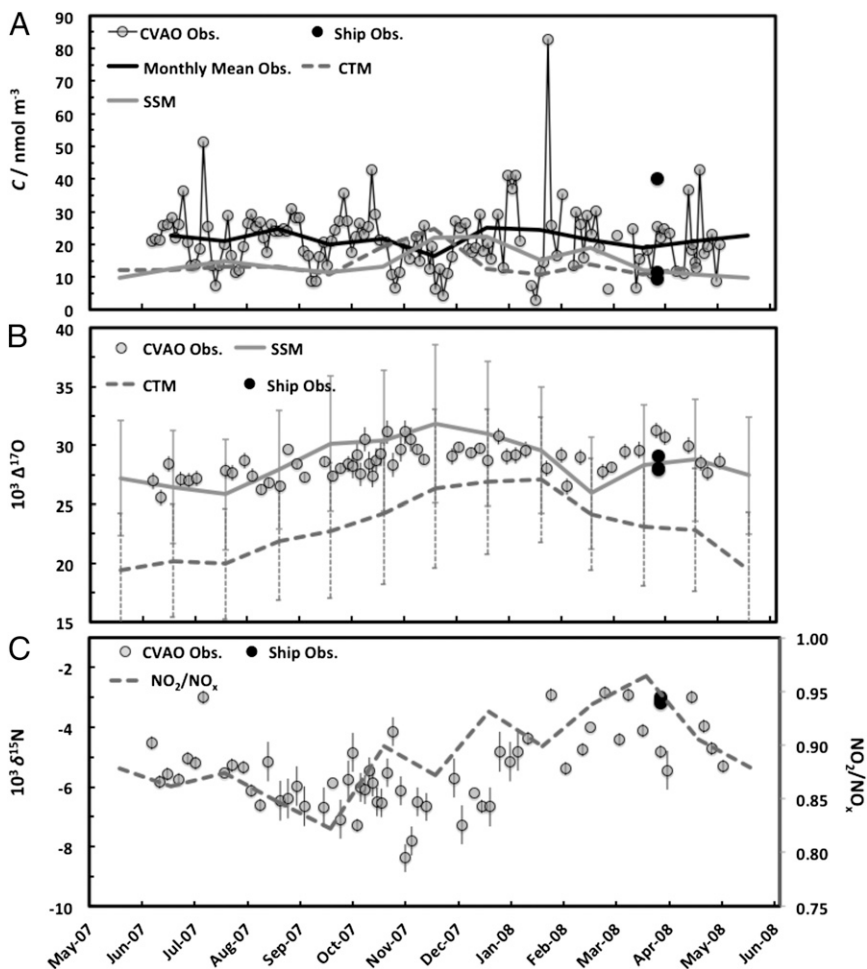
Fig. 1. Observed concentration (*A*), $\Delta^{17}O$ (*B*), and $\delta^{15}N$ (*C*) of atmospheric nitrate collected at the CVAO (CVAO Obs.). Also displayed are the measurements performed on three different cruises (2007, 2008, and 2012) onboard the R/V *Polarstern* (Ship Obs.) when sailing in the vicinity of Cape Verde. The monthly average and predicted concentrations by the SSM and the CTM are shown in *A*, and predicted $\Delta^{17}O$ values, including BrNO$_3$ chemistry for the SSM, are shown in *B*. (*C*) NO$_2$/NO$_x$ ratio as obtained by local NO$_x$ measurements.

Table 1. Comparison of the seasonal minimum and maximum values of nitrate isotope ratios at different locations

Location	$10^3 \Delta^{17}O$		$10^3 \delta^{15}N$	
	Minimum	Maximum	Minimum	Maximum
Tropic Atlantic (Cape Verde, 17° N)	+27 (Jul)	+31 (Dec)	−8 (Oct)	−2 (Mar)
Polar (Alert, 82° N)* (13)	+24 (Jul)	+32 (Dec)	−1 (Aug)	−15 (Dec)
Polar (Barrow, 71° N)* (27)	+21 (Jun)	+28 (Sep)	−1 (Aug)	−10 (Nov)
Red Sea (Gulf of Aqaba, 30° N) (26)			−4 (Oct)	+2 (Aug)
Pacific coastal (San Diego, 33° N) (7)	+21 (Jul)	+30 (Jan)		

Abbreviations for the months of the observed minimum and maximum are shown in parentheses.
*Values are given for the general seasonal trend, excluding the springtime due to the occurrence of ozone depletion events.

Discussion

Framework. Our $\Delta^{17}O$ and $\delta^{15}N$ datasets represent a tentative to connect the isotopic composition of atmospheric nitrate with the reactive chemistry in the tropical MBL. Recently, Morin et al. (15) conducted an extensive analysis of the ^{17}O-excess transfer from the $O_x/HO_x/NO_x$ families to atmospheric nitrate in different atmospheric contexts, extending the initial work of Michalski et al. (7) by introducing the diurnally integrated isotopic signature (DIIS) metric (*Materials and Methods*). Such studies provide the quantification tools to compare directly the outputs of an atmospheric chemistry model with the observed $\Delta^{17}O$ of atmospheric nitrate (helped by $\delta^{15}N$ in some situations), bringing a new set of constraint on the chemical processes occurring in the atmosphere beyond the solely concentration measurements (12, 13, 17, 18). In the present study, a chemical box model (SSM) and a 3D model (CTM) are confronted with the CVAO observations, first with the observed concentrations and then with the stable oxygen isotope compositions.

Observed and Modeled Concentrations. To allow for a consistent comparison between models and observations, the lifetime of atmospheric nitrate in the SSM was set to the same value as in the CTM (i.e., 3.5 d). Under such conditions, the SSM and the CTM predicted similar nitrate concentrations, indicating that the total production rate of nitrate in both models was approximately equal. Considering the uncertainty associated with the kinetic rates and concentrations of the prescribed reactive species (at least 30% for each term), the models quantitatively predicted the nitrate concentrations within a factor of 2 (Fig. 1*A*). Although the models appeared to calculate a more pronounced seasonality than the observations, it is probably insignificant considering the large uncertainty. On the other hand, the identical concentrations predicted by both models strongly support the premise that the prevailing marine conditions at the CVAO are also valid for the air masses transported to this site, in agreement with recent studies (23, 27), making our observed seasonal trends weakly sensitive to transport and air mass origin. The best concentration match between observations and model predictions was actually found for a nitrate lifetime of *ca.* 5 d. Statistical analysis of 5-d back-trajectories of air masses reaching the CVAO indicated that they were essentially marine air with little continental origin, making the CVAO representative of the wider North Atlantic MBL (28). The air mass dynamics are therefore compatible with a local approach and, with a lifetime significantly greater than 1 d, validated the use of the DIIS [i.e., $\Delta^{17}O$ depends only on the relative strength of each reaction pathway weighted by its respective DIIS (Fig. S2); thus it is insensitive to any atmospheric sinks] (15).

Modeled Chemistry. The concentrations predicted by the models are the results of their internal chemistry. A closer look at individual production pathways (Fig. 2 and Table S2) reveals fundamental differences between the models. Although displaying almost identical concentration time series that are in good

agreement with the observations, they used different reaction schemes. For the CTM, NO + OH largely dominated the formation of nitrate ($P_{NO2+OH} \approx 70\%$ on average), with significant production from N_2O_5 hydrolysis ($P_{N2O5+H2O}$ up to 30%). For the SSM, $P_{N2O5+H2O}$ was negligible, whereas the other pathways were nearly equal (20–40%; Fig. 2). Although these percentages should be taken with caution due to their inherent uncertainty (at least ± 50% of the values), they reveal the different reaction chemistries used by the models.

It is interesting to note that these chemistries, although predicting almost the same atmospheric nitrate concentrations, differed greatly when $\Delta^{17}O$ was concerned. Indeed, such discrepancies in chemistry translated into important differences in predicted $\Delta^{17}O$ of nitrate (Fig. 1*B*), because each reaction pathway carries a specific $\Delta^{17}O$ value (Fig. S2). It is obvious from Fig. 1*B* that the SSM is in better agreement with the observed $\Delta^{17}O$, giving more credence to its chemistry than the CTM. Considering that the SSM is constrained by observations, its main weakness (the transport) had little effect on ^{17}O-excess transfer (homogeneous MBL at the spatial scale of the atmospheric lifetime) and it better reproduced the observed $\Delta^{17}O$ of nitrate; thus, we consider the SSM model to be a better representation of the atmospheric chemistry operating
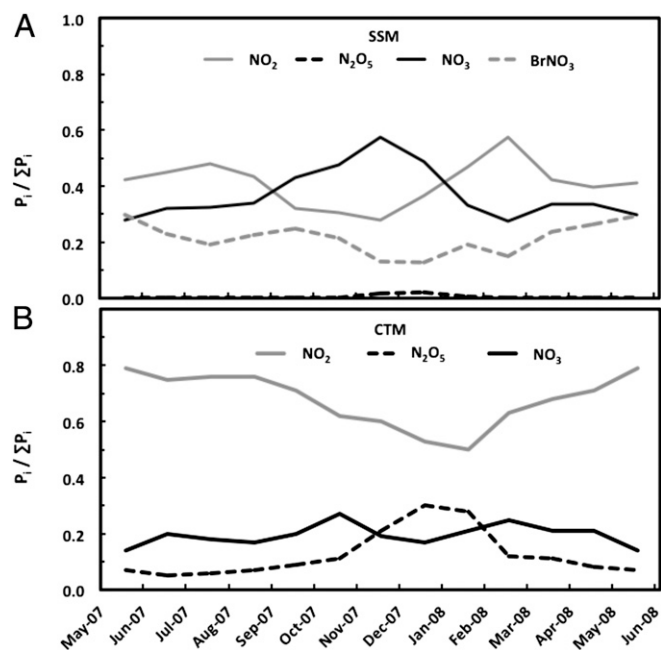
Fig. 2. Relative production rates of atmospheric nitrate by each oxidation pathway ($NO_2 + OH$, $NO_3 + VOC$, $N_2O_5 + H_2O$, and $BrNO_3 + H_2O$), leading to the formation of atmospheric nitrate. The SSM (*A*) and CTM (*B*), respectively, are shown.

at the CVAO and discuss first its results before comparing them with the CTM results.

SSM Features. One of the most striking features of the SSM output was the relative low importance attributed to the N_2O_5 reaction channel. Recently, questions have emerged regarding the role of N_2O_5 in models, especially in the clean marine atmosphere (5, 6, 29). These studies generally point to an overestimation of the uptake coefficient of N_2O_5 (30). However, in the present case, sensitivity tests showed that the SSM was unaffected by three orders of magnitude changes in the N_2O_5 uptake coefficient (range: 10^{-3} to 1). The weak sensitivity on the uptake coefficient of N_2O_5 resulted directly from the very low concentration of NO_x observed at the CVAO (tens of pmol·mol^{-1}) (22), preventing significant nighttime N_2O_5 formation via its thermal equilibrium $N_2O_5 \leftrightarrow NO_3 + NO_2$. The lack of N_2O_5 formation also excludes the $2NO_2 + NaCl \rightarrow ClNO + HNO_3$ reaction as a significant source of atmospheric nitrate. The formation of HNO_3 via this reaction has been found to be quadratic in NO_2 pressure with an uptake coefficient in the range of 10^{-5} (31), making this reaction even less probable than N_2O_5 in the poor NO_x environment of the CVAO. These conclusions are supported by other studies modeling the pristine MBL (32, 33). A direct consequence of the very low N_2O_5 concentration was the absence of nitryl compounds (e.g., $ClNO_2$, $BrNO_2$) (32) produced by the interaction of N_2O_5 with halides (NaI, NaBr, and NaCl) (34). Moreover, the predominance of the nighttime $P_{NO3+DMS}$ (Fig. 2) during winter, even surpassing the daytime P_{NO2+OH} as the main NO_x sink, was found to be in agreement with previous studies (30, 33). $P_{NO3+DMS}$ gave rise to the $\Delta^{17}O$ winter peak in the SSM. This situation differs from more polluted environments, where N_2O_5 played a pivotal role (30).

A remarkable feature of the $\Delta^{17}O$ variations recorded at the CVAO was the high $\Delta^{17}O$ values observed in summer relative to other locations worldwide (Table 1). As indicated in Fig. 1B, the SSM reproduced the summer observations relatively well within 1‰ in contrast to the CTM, which underestimated the observations by ≈5‰. The high summer values were obtained as a result of the relatively high ^{17}O-excess transfer by the BrO chemistry (Fig. S2). This is further demonstrated by switching off the bromine chemistry in the SSM, which degraded by 2–3‰ the agreement between observations and model results in summer (Fig. S3). It is known that the bromine chemistry has a significant impact on the $\Delta^{17}O$ signature of atmospheric nitrate in the polar atmosphere because $BrNO_3$ possesses the same $\Delta^{17}O$ as NO_3 (BrO inherits its transferable O-atom from ozone, making the reactions $NO_2 + BrO$ and $NO_2 + O_3$ equivalent but different from $NO_2 + OH$ because OH includes an O-atom inherited from H_2O) (13). Near-constant BrO concentrations of ca. 2.5 pmol·mol^{-1} year-round have been observed at the CVAO (3, 35). BrO can have an impact on the $\Delta^{17}O(NO_3^-)$ signature through NO_2 formation ($NO + BrO \rightarrow NO_2 + Br$) and $BrNO_3$ hydrolysis on wet solid surfaces ($BrNO_3 + H_2O \rightarrow HOBr + HNO_3$) (Fig. S1). Calculations using local mole ratios and the kinetic constant for the $NO + BrO$ reaction showed little impact of this reaction on $\Delta^{17}O(NO_2)$ [+0.5‰ at maximum for $\Delta^{17}O(NO_3^-)$] because $NO + O_3$ still dominates the oxidation of NO (Table S3). More difficult, however, is an assessment of the impact of heterogeneous XNO_3 hydrolysis reactions (with X representing Cl, Br, or I) on $\Delta^{17}O(NO_3^-)$ because $ClNO_3$ and INO_3 can also potentially contribute to nitrate formation in the marine atmosphere (32, 34). Although ca. 1 pmol·mol^{-1} of iodine monoxide (IO) has been measured at the CVAO (3), there are no available observations for chlorine monoxide (ClO). A halogen chemistry model applied to the pristine CVAO environments predicts ClO values in the range of 2 pmol·mol^{-1} (32), making the total mole ratio of XO about twice the observed BrO concentration. Treating the sum of XO as a surplus of BrO [XO + NO_2 have an almost identical reaction rate constant and oxidation mechanism (34, 36)], a sensitivity test shows that doubling the halogen production rate from 5.7 to 11.4 × 10^3 molecules per cm^{-3}·s^{-1} increases the predicted $\Delta^{17}O$ by 2‰ and increases the relative

reaction rate of the halogen chemistry by ca. +10%, which does not fundamentally alter our interpretation. If only $BrNO_3$ is considered, the $BrNO_3$ pathway accounts for an average HNO_3 production of 20 ± 10% with a seasonality of ca. 10% and 30% for winter and summer, respectively [the seasonality has been introduced by variation of the other production rates because the BrO mole ratio displayed no seasonal variation (3)]. Uncertainty in this estimation is constrained by the isotope mass balance (not the concentration) and clearly indicates that an absence of halogen chemistry significantly degrades the predicted $\Delta^{17}O$ composition. It should also be noted that the $\Delta^{17}O$ used for ozone has no impact on this estimation because all ^{17}O-excess transfer mechanisms scale identically with this parameter (15), thus conserving the $\Delta^{17}O$ seasonality. Nevertheless, in this study, we used $\Delta^{17}O(O_3)$ measured in the vicinity of the CVAO, applying our unique analytical approach (37), and thus did not adjust this variable to match the observed $\Delta^{17}O$, in contrast to previous studies (7, 12, 13, 18).

CTM Features. Using the SSM as a benchmark, several conclusions may be drawn regarding the CTM. Although the CTM displayed the same seasonal amplitude as the SSM, it underestimated the $\Delta^{17}O$ of NO_3^- for all seasons. Because both models use the same isotope mechanism [i.e., DIIS and $\Delta^{17}O(O_3)$], the difference was clearly in the chemistry. Compared with the SSM (Fig. 2), the CTM largely favored its daytime chemistry (i.e., $NO_2 + OH$), placing too much emphasis on the N_2O_5 hydrolysis and not enough on the NO_3 pathways. A difference in DMS concentration can be excluded because the CTM used greater DMS concentrations than the SSM (on average, 200 pmol·mol^{-1} in summer for the CTM compared with 30 pmol·mol^{-1} for the SSM). It is evident that all these differences are interlinked via the radical chemistry; thus, it is difficult to pinpoint a principal weakness. The lack of the halogen chemistry is likely an important cause, given the strong influence this chemistry can exert on the O_x, HO_x, and NO_x families (34), but it is clearly not the only one (only 2–3‰ of 5‰ is quantitatively explained by the halogen chemistry). If the transport is suppressed in the CTM, N_2O_5 chemistry becomes unimportant (as in the SSM) and the formation of nitrate is almost equally split between $NO_2 + OH$ (identical to the SSM) and NO_3 (twice that of the SSM). The result is a predicted $\Delta^{17}O$ that is as good as that in the SSM but for the wrong reasons. In this situation, the increase of the nighttime NO_3 chemistry produced an increase in $\Delta^{17}O$ that compensated for the lack of the halogen chemistry because both have the same ^{17}O-excess transfer function. Thus, the importance of the N_2O_5 chemistry in the CTM was clearly the result of the history of the air mass, which tended to degrade the predicted $\Delta^{17}O$ significantly, either through the NO_x source implementation or the calculated uptake coefficient.

Summary and Conclusion

In this study, we have reported the annual time series of the $\Delta^{17}O$ and $\delta^{15}N$ values of atmospheric nitrate at a tropical MBL location. Studies in the tropical MBL are fundamental for an understanding of the oxidation capacity of the atmosphere, given the important role played by this region in global atmospheric chemistry. Using the transfer model developed by Morin et al. (15), fed with aerosol surface area measurements, and the local mole ratios of BrO, NO, NO_2, O_3, OH, HO_2, and DMS, we have modeled the $\Delta^{17}O$ of atmospheric nitrate. The predicted seasonal time series of $\Delta^{17}O$ indicated that the atmospheric nitrate reaching the CVAO is largely representative of an area equivalent to a few days of aerosol transport in the remote marine atmosphere. Furthermore, the reactive halogen chemistry in the tropical MBL was compatible with the observed $\Delta^{17}O$ of atmospheric nitrate, with a nitrate production rate of 20 ± 10% (ca. 10% and 30% for winter and summer, respectively) for this reaction pathway. The low concentration of NO_x in this environment precluded the formation of N_2O_5 and its reaction products, especially the nitryl halogen compounds (e.g., $ClNO_2$). A recent

controversy regarding the role of N_2O_5 as a sink of NO_x has emerged, with proposed uptake coefficient values varying by orders of magnitude (e.g., ref. 5). In this regard, our $\Delta^{17}O(NO_3^-)$ measurements are incompatible with a high production rate of HNO_3 from N_2O_5 hydrolysis, in agreement with studies that have suggested a substantially reduced magnitude of the NO_x sink from N_2O_5 for clean environments (5, 33, 38). It is possible that for the remote marine atmosphere, the lack of halogen chemistry implementation in models has led to an overestimation of the N_2O_5 pathway (39). Because oxidation chemistry in the atmosphere involves a transfer of oxygen atoms, stable oxygen isotope ratios are particularly useful tools for following such chemistry, as demonstrated in the present work. In this perspective, the surprisingly high oxidation capacity found in tropical forests (40) provides another environment in which the $\Delta^{17}O$ metric may provide new insights. Here, an unexplained high OH production rate in a low NO_x and high VOC environment was observed. This environment should result in the lowest atmospheric $\Delta^{17}O$ (NO_3^-) signatures. $\delta^{15}N$ is found to be more difficult to interpret, apparently due to a predominantly local control on ^{15}N partitioning between nitrogen species. Close examination with previous studies indicated that the annual variations in ^{15}N in this tropical marine atmosphere were driven by a different mechanism than that observed at higher northern latitudes. A covariation of $\delta^{15}N$ with NO_2/NO_x ratio is suggested, but in the opposite direction of previous studies in air masses affected by urban and industrial emissions. We hypothesize that this seasonality is probably driven by the partition of NO_x species between NO and NO_2. Measuring ^{15}N of NO and NO_2 should help in solving this uncertainty (41).

Materials and Methods

Definitions. Conventionally, δ is defined as (42):

$$\delta^x Y_{spl/ref} = \frac{^x R_{spl}}{^x R_{ref}} - 1 \qquad [1]$$

where $^x R$ represents the mole ratio $n(^{17}O)/n(^{16}O)$, $n(^{18}O)/n(^{16}O)$, or $n(^{15}N)/n(^{14}N)$ in the sample (spl) and reference (ref), respectively, and $^x Y$ is the respective isotope. The references for oxygen and nitrogen are Vienna standard mean ocean water and atmospheric N_2, respectively (ref. 43 and references therein). For practical reasons, δ values are generally expressed in per mill (‰), because variations in isotopic ratios cover a very narrow range of values.

^{17}O-excess is expressed here by its linear definition, where $\Delta^{17}O = \delta^{17}O - 0.52 \times \delta^{18}O$. The δ values are reported against their respective international reference scale.

Sampling and Analysis. Bulk aerosol samples were collected from a 30-m-high observation tower located on the island of São Vicente, Cape Verde Island (16° 51′ 49″ N, 24° 52′ 02″ W) in the period from July 3, 2007 through May 29, 2008. Samples were collected on 47-mm, 0.4-μm polypropylene filters (Sterlitech). Air sampling was conducted using a low-volume aerosol collection system, which pumps at a rate of ~30 L/min. Mass flow meters were used to measure the volume of air pumped over the filters. The filters were collected and replaced every 48–72 h. Collected filters containing atmospheric aerosols were stored at −20 °C until extraction and analysis.
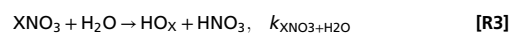
Soluble species deposited on the filters were extracted in 100 mL of ultrapure water (18 MΩ·cm^{-1}) under ultraclean conditions (44). All subsequent analyses were performed on the nitrate dissolved during this step. Nitrate concentrations were determined in filter extracts using ion chromatography, with a reported uncertainty of ~5% in the range of 1–1,000 ng·g^{-1} (45). Atmospheric concentrations were calculated by dividing the mass of nitrate recovered on the filters by the total sampled air volume (no correction for standard pressure and temperature was applied). The contribution of sampling blanks was always found to be negligible. Nitrogen and oxygen isotope ratios were measured using an automated denitrifier method as described by Morin et al. (27). This technique uses *Pseudomonas aureofaciens* bacteria to convert nitrate to N_2O, which is then analyzed for its isotopic composition after thermal decomposition to O_2 and N_2 in a gold tube (46). The analytical procedure used for this study is strictly identical to the description given by Morin et al. (27). Isotopic analysis was performed on a Thermo Finnigan MAT253 (continuous flow mode) equipped with a gas-bench interface.

Uncertainties pertaining to the $\delta^{18}O$, $\Delta^{17}O$, and $\delta^{15}N$ values are ca. ±1.8‰, ±0.5‰, and ±0.4‰, on average, respectively.
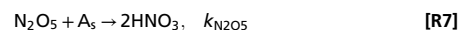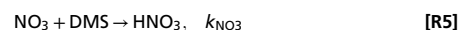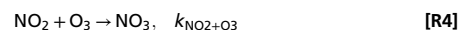
Method. *Chemistry and isotopes.* The interpretive framework that has been developed for the quantitative evaluation of the $\Delta^{17}O$ of NO_3^- in terms of its production pathways follows from conservation of mass applied to $\Delta^{17}O$ and is based on the simple idea of tracing the origin of oxygen atoms transferred from reactants to products (15). In the majority of cases, the following reactions are sufficient to interpret $\Delta^{17}O$ (7) (Fig. S1). During the day, the majority of atmospheric nitrate is formed via the following reactions (R):

$$NO_2 + OH \rightarrow HNO_3, \quad k_{NO2+OH} \qquad [R1]$$

In certain situations in which halogen concentrations are significant, the following reactions will compete with OH (with X representing Cl, Br, or ionium):

$$NO_2 + XO \rightarrow XNO_3, \quad k_{NO2+XO} \qquad [R2]$$

$$XNO_3 + H_2O \rightarrow HO_X + HNO_3, \quad k_{XNO3+H2O} \qquad [R3]$$

At night, in a remote marine atmosphere where DMS (CH_3SCH_3) dominates over VOCs, the formation of higher nitrogen oxides drives the chemistry of nitrate:

$$NO_2 + O_3 \rightarrow NO_3, \quad k_{NO2+O3} \qquad [R4]$$

$$NO_3 + DMS \rightarrow HNO_3, \quad k_{NO3} \qquad [R5]$$

$$NO_3 + NO_2 \leftrightarrow N_2O_5, \quad K_{eq} \qquad [R6]$$

$$N_2O_5 + A_s \rightarrow 2HNO_3, \quad k_{N2O5} \qquad [R7]$$

where A_s symbolizes a hydrated aerosol surface area concentration (square micrometers per cubic centimeter) for the heterogeneous R7 reaction (4). To predict the $\Delta^{17}O$ of NO_3^- produced by the above chemistry, we used the formalism developed by Morin et al. (15) under the assumption that the atmospheric lifetime of NO_3^- is significantly longer than 1 d, a condition fulfilled at the CVAO (47, 48). The modeled monthly mean $\Delta^{17}O$ of nitrate is then expressed (*SI Text*):

$$\Delta^{17}O(NO_3^-) = \frac{\sum_i \left(P_i \times \overline{\Delta^{17}O(NO_3^-)} \right)}{\sum_i P_i} \qquad [2]$$

where $\overline{\Delta^{17}O(NO_3^-)}$ and P_i represent the DIIS (no unit) and the chemical production rate (molecules per cubic centimeter per second of nitrate), respectively. We used the explicit seasonal DIIS for each P_i as modeled by Morin et al. (15) for 45° N, which implicitly integrates seasonal variations in the $\Delta^{17}O$ of NO_2. Tests show that the DIISs are not very sensitive to the latitude, with a notable exception at polar latitudes. We have scaled the transfer functions to a transferrable ^{17}O-excess [$\Delta^{17}O(O_3^*)$] of 40‰, a value obtained using a newly developed analytical method (37) in the vicinity of Cape Verde during the 2012 ANTXXVIII/5 cruise of the R/V *Polarstern*, obtained with an analytical SD of ±3‰. Note that the predicted values of any model calculation dependent strongly on the scenario used for $\Delta^{17}O$ (O_3^*) (15). We adopted a constant value because ^{17}O-excess ozone is not expected to change greatly in the troposphere due to its low sensitivity to pressure and temperature (49). The quantitative results provided in this report would need to be reconsidered should $\Delta^{17}O(O_3^*)$ be found to exhibit significant diurnal or seasonal variability.

SSM. Concentrations of oxidants (OH, HO$_2$, BrO, and O$_3$), DMS, aerosols, and NO_x were used to calculate the production rate of each pathway (R1, R3, R5, and R7) leading to nitrate formation (i.e., P_{NO2+OH}, $P_{XNO3+H2O}$, $P_{NO3+DMS}$, $P_{N2O5+As}$, respectively; details are provided in *SI Text*) (Fig. S1). These production rates then served as input in an isotope mass balance model used to calculate $\Delta^{17}O$ (15). The models generate the relative nitrate production rate (Fig. 2) and the individual $\Delta^{17}O$ of each nitrate production channel (Fig. S2) and, via summation, provided the predicted $\Delta^{17}O(NO_3^-)$ (Fig. 1B).

The uncertainty of the predicted $\Delta^{17}O$ is calculated using the quadratic sum of the individual variables, which includes the production rate and the DIIS. For the production rate, a relative uncertainty of 30% is assumed, representing the general uncertainties of the kinetic rates and the concentration measurements. For the DIIS, the variability range of individual DIISs is extracted from the different scenarios described in the work of

Morin et al. (15). The relative uncertainty of the individual DIISs never exceeds 10%.

CTM. The same exercise was conducted using the global 3D GEOS-Chem CTM to obtain the monthly "transported" P_i (i.e., P_{NO2+OH}, $P_{NO3+DMS}$, $P_{N2O5+As}$) while keeping the same DIIS used in the SSM (Figs. 1B and 2 and Fig. S2). The version of the CTM used in this study does not include halogen chemistry, such as the formation of atmospheric nitrate via $BrNO_3$ hydrolysis. Details of the CTM model can be found in the study by Alexander et al. (18). We applied the same $\Delta^{17}O$ uncertainty to the 3D CTM as calculated for the SSM.

1. Bloss WJ, et al. (2005) The oxidative capacity of the troposphere: Coupling of field measurements of OH and a global chemistry transport model. *Faraday Discuss* 130:425–436; discussion 491–517, 519–424.
2. Lelieveld J, Dentener FJ (2000) What controls tropospheric ozone? *J Geophys Res* 105(D3):3531–3551.
3. Read KA, et al. (2008) Extensive halogen-mediated ozone destruction over the tropical Atlantic Ocean. *Nature* 453(7199):1232–1235.
4. Finlayson-Pitts BJ, Pitts JN (2000) *Chemistry of the Upper and Lower Atmosphere: Theory, Experiments and Applications* (Academic, San Diego).
5. Brown SS, et al. (2009) Reactive uptake coefficients for N_2O_5 determined from aircraft measurements during the Second Texas Air Quality Study: Comparison to current model parameterizations. *J Geophys Res* 114:D00F10, 10.1029/2008jd011679.
6. Brown SS, et al. (2006) Variability in nocturnal nitrogen oxide processing and its role in regional air quality. *Science* 311(5757):67–70.
7. Michalski G, Scott Z, Kabiling M, Thiemens MH (2003) First measurements and modeling of $\Delta^{17}O$ in atmospheric nitrate. *Geophys Res Lett* 30(16):1870, 10.1029/2003gl017015.
8. Kendall C, Elliott EM, Wankel SD (2007) *Tracing Anthropogenic Inputs of Nitrogen to Ecosystems. Stable Isotopes in Ecology and Environmental Science* (Blackwell, Oxford), 2nd Ed.
9. Michalski G, Bhattacharya SK, Mase DF (2012) Oxygen isotope dynamics of atmospheric nitrate. *Handbook of Environmental Isotope Geochemistry*, ed Baskaran M (Springer, Heidelberg), pp 613–637.
10. Savarino J, Morin S (2012) The N, O, S isotopes of oxy-anions in ice core and polar environments. *Handbook of Environmental Isotope Geochemistry*, ed Baskaran M (Springer, Heidelberg), pp 835–864.
11. Hastings MG, Sigman DM, Lipschultz F (2003) Isotopic evidence for source changes of nitrate in rain at Bermuda. *J Geophys Res* 108(D24):4790, 10.1029/2003jd003789.
12. Savarino J, Kaiser J, Morin S, Sigman DM, Thiemens MH (2007) Nitrogen and oxygen isotopic constraints on the origin of atmospheric nitrate in coastal Antarctica. *Atmos Chem Phys* 7:1925–1945, 10.5194/acp-7-1925-2007.
13. Morin S, et al. (2008) Tracing the origin and fate of NOx in the Arctic atmosphere using stable isotopes in nitrate. *Science* 322(5902):730–732.
14. Jarvis JC, Hastings MG, Steig EJ, Kunasek SA (2009) Isotopic ratios in gas-phase HNO_3 and snow nitrate at Summit, Greenland. *J Geophys Res* 114(D17):D17301, 10.1029/2009jd012134.
15. Morin S, Sander R, Savarino J (2011) Simulation of the diurnal variations of the oxygen isotope anomaly ($\Delta^{17}O$) of reactive atmospheric species. *Atmos Chem Phys* 11(8):3653–3671.
16. McCabe JR, Thiemens MH, Savarino J (2007) A record of ozone variability in South Pole Antarctic snow: Role of nitrate oxygen isotopes. *J Geophys Res* 112(D12):D12303, 10.1029/2006jd007822.
17. Kunasek SA, et al. (2008) Measurements and modeling of $\Delta^{17}O$ of nitrate in snowpits from Summit, Greenland. *J Geophys Res* 113(D24):D24302, 10.1029/2008jd010103.
18. Alexander B, et al. (2009) Quantifying atmospheric nitrate formation pathways based on a global model of the oxygen isotopic composition ($\Delta^{17}O$) of atmospheric nitrate. *Atmos Chem Phys* 9:5043–5056, 10.5194/acp-9-5043-2009.
19. Freyer HD, Kley D, Volz-Thomas A, Kobel K (1993) On the interaction of isotopic exchange processes with photochemical reactions in atmospheric oxides of nitrogen. *J Geophys Res* 98(D8):14791–14796.
20. Elliott EM, et al. (2009) Dual nitrate isotopes in dry deposition: Utility for partitioning NOx source contributions to landscape nitrogen deposition. *J Geophys Res* 114(G4):G04020, 10.1029/2008jg000889.
21. Freyer HD (1991) Seasonal variation of $^{15}N/^{14}N$ ratios in atmospheric nitrate species. *Tellus B Chem Phys Meterol* 43(1):30–44.
22. Lee JD, et al. (2009) Year-round measurements of nitrogen oxides and ozone in the tropical North Atlantic marine boundary layer. *J Geophys Res* 114:D21302, 10.1029/2009jd011878.
23. Carpenter LJ, et al. (2010) Seasonal characteristics of tropical marine boundary layer air measured at the Cape Verde Atmospheric Observatory. *J Atmos Chem* 67(2-3):87–140.
24. Buda AR, DeWalle DR (2009) Using atmospheric chemistry and storm track information to explain the variation of nitrate stable isotopes in precipitation at a site in central Pennsylvania, USA. *Atmos Environ* 43(29):4453–4464.
25. Wankel SD, Chen Y, Kendall C, Post AF, Paytan A (2010) Sources of aerosol nitrate to the Gulf of Aqaba: Evidence from $\delta^{15}N$ and $\delta^{18}O$ of nitrate and trace metal chemistry. *Mar Chem* 120(1-4):90–99.
26. Morin S, et al. (2012) An isotopic view on the connection between photolytic emissions of NOx from the Arctic snowpack and its oxidation by reactive halogens. *J Geophys Res* 117:D00R08, 10.1029/2011jd016618.
27. Morin S, et al. (2009) Comprehensive isotopic composition of atmospheric nitrate in the Atlantic Ocean boundary layer from 65°S to 79°N. *J Geophys Res* 114(D5):D05303, 10.1029/2008jd010696.
28. Lee JD, et al. (2010) Reactive Halogens in the Marine Boundary Layer (RHaMBLe): The tropical North Atlantic experiments. *Atmos Chem Phys* 10(3):1031–1055.
29. Bertram TH, et al. (2009) Direct observations of N2O5 reactivity on ambient aerosol particles. *Geophys Res Lett* 36(19):L19803, 10.1029/2009gl040248.
30. Brown SS, Stutz J (2012) Nighttime radical observations and chemistry. *Chem Soc Rev* 41(19):6405–6447.
31. Li H, Zhu T, Ding J, Chen Q, Xu B (2006) Heterogeneous reaction of NO_2 on the surface of NaCl particles. *Sciences in China series B. Chemistry* 49(9):371–378.
32. Sommariva R, von Glasow R (2012) Multiphase halogen chemistry in the tropical Atlantic Ocean. *Environ Sci Technol* 46(19):10429–10437.
33. Allan BJ, McFiggans G, Plane JMC, Coe H, McFadyen GG (2000) The nitrate radical in the remote marine boundary layer. *J Geophys Res* 105(D19):24191–24204.
34. Saiz-Lopez A, von Glasow R (2012) Reactive halogen chemistry in the troposphere. *Chem Soc Rev* 41(19):6448–6472.
35. Mahajan AS, et al. (2010) Measurement and modelling of tropospheric reactive halogen species over the tropical Atlantic Ocean. *Atmos Chem Phys* 10(10):4611–4624.
36. Atkinson R, et al. (2007) Evaluated kinetic and photochemical data for atmospheric chemistry: Volume III—Gas phase reactions of inorganic halogens. *Atmos Chem Phys* 7(4):981–1191.
37. Vicars WC, Bhattacharya SK, Erbland J, Savarino J (2012) Measurement of the ^{17}O-excess ($\Delta^{17}O$) of tropospheric ozone using a nitrite-coated filter. *Rapid Commun Mass Spectrom* 26(10):1219–1231.
38. Davis JM, Bhave PV, Foley KM (2008) Parameterization of N2O5 reaction probabilities on the surface of particles containing ammonium, sulfate, and nitrate. *Atmos Chem Phys* 8(17):5295–5311.
39. Sander R, Rudich Y, von Glasow R, Crutzen PJ (1999) The role of $BrNO_3$ in marine tropospheric chemistry: A model study. *Geophys Res Lett* 26(18):2857–2860.
40. Lelieveld J, et al. (2008) Atmospheric oxidation capacity sustained by a tropical forest. *Nature* 452(7188):737–740.
41. Smirnoff A, Savard MM, Vet R, Simard M-C (2012) Nitrogen and triple oxygen isotopes in near-road air samples using chemical conversion and thermal decomposition. *Rapid Commun Mass Spectrom* 26(23):2791–2804.
42. Coplen TB (2011) Guidelines and recommended terms for expression of stable-isotope-ratio and gas-ratio measurement results. *Rapid Commun Mass Spectrom* 25(17):2538–2560.
43. Böhlke JK, Mroczkowski SJ, Coplen TB (2003) Oxygen isotopes in nitrate: New reference materials for $^{18}O{:}^{17}O{:}^{16}O$ measurements and observations on nitrate-water equilibration. *Rapid Commun Mass Spectrom* 17(16):1835–1846.
44. Morin S, Savarino J, Bekki S, Gong S, Bottenheim JW (2007) Signature of Arctic surface ozone depletion events in the isotope anomaly ($\Delta^{17}O$) of atmospheric nitrate. *Atmos Chem Phys* 7:1451–1469, 10.5194/acp-7-1451-2007.
45. Preunkert S, Wagenbach D, Legrand M (2003) A seasonally resolved alpine ice core record of nitrate: Comparison with anthropogenic inventories and estimation of preindustrial emissions of NO in Europe. *J Geophys Res* 108(D21):4681, 10.1029/2003jd003475.
46. Kaiser J, Hastings MG, Houlton BZ, Röckmann T, Sigman DM (2007) Triple oxygen isotope analysis of nitrate using the denitrifier method and thermal decomposition of N2O. *Anal Chem* 79(2):599–607.
47. Lawler MJ, et al. (2009) Pollution-enhanced reactive chlorine chemistry in the eastern tropical Atlantic boundary layer. *Geophys Res Lett* 36:L08810, 10.1029/2008gl036666.
48. Muller K, et al. (2010) Particle characterization at the Cape Verde atmospheric observatory during the 2007 RHaMBLe intensive. *Atmos Chem Phys* 10(6):2709–2721.
49. Morton J, Barnes J, Schueler B, Mauersberger K (1990) Laboratory studies of heavy ozone. *J Geophys Res* 95(D1):901–907.